RESEARCH ARTICLE

Graphene/Carbon Based Materials

Energy & Environmental Materials WILEY

Highly Flexible Graphene-Film-Based Rectenna for Wireless Energy Harvesting

Jingwei Zhang, Yuchao Wang, Rongguo Song, Zongkui Kou, and Daping He**

Herein, we report the design, fabrication, and performance of two wireless energy harvesting devices based on highly flexible graphene macroscopic films (FGMFs). We first demonstrate that benefiting from the high conductivity of up to 1×10^6 S m^{-1} and good resistive stability of FGMFs even under extensive bending, the FGMFs-based rectifying circuit (GRC) exhibits good flexibility and RF-to-DC efficiency of 53% at 2.1 GHz. Moreover, we further expand the application of FGMFs to a flexible wideband monopole rectenna and a 2.45 GHz wearable rectenna for harvesting wireless energy. The wideband rectenna at various bending conditions produces a maximum conversion efficiency of 52%, 46%, and 44% at the 5th Generation (5G) 2.1 GHz, Industrial Long-Term Evolution (LTE) 2.3 GHz, and Scientific Medical (ISM) 2.45 GHz, respectively. A 2.45 GHz GRC is optimized and integrated with an AMC-backed wearable antenna. The proposed 2.45 GHz wearable rectenna shows a maximum conversion efficiency of 55.7%. All the results indicate that the highly flexible graphene-film-based rectennas have great potential as a wireless power supplier for smart Internet of Things (IoT) applications.

1. Introduction

Nowadays, the Internet of Things (IoT) interconnects a vast number of objects (e.g., mobile devices, smart electronics) equipped with pervasive wireless sensors to enable automat, ambient-living, real-time data monitoring, and remote control.[1,2] Since they typically need batteries that must be maintained and replaced, the design and realization of the compact, energy-autonomous, self-powered system are highly desired in IoT applications. Currently, wireless energy, as a renewable wireless source, is becoming a potential solution for low-power IoT applications due to its unique advantage of high anti-environmental climate interference ability. With the rapid development of the wireless industry, energy harvesting from wireless power has been a hot research area.[3–8] Depending on the increasing number of mobile cellular networks and Wi-Fi-enabled applications, ambient microwave energy is dramatically increasing and ubiquitous in indoor and outdoor environments. The wireless power can be harvested and converted to direct current (DC) by a rectenna (a portmanteau of rectifying antenna) that can be regarded as a power supplier for batteryless sensors and smart devices.[9–11]

The rectenna for wireless energy harvesting has been investigated for over a decade, mainly focusing on improving the harvested DC power or conversion efficiency under different scenarios,[12–14] and some hybrid energy (wireless and solar power) harvesting batteryless devices have been produced, such as a batteryless camera[15] and a battery-free cellphone.[16] However, with the increasing number of flexible electronics widely utilized in IoT, smart cities, and smart health applications.[17–19] As a power supplier, the rectenna used in flexible electronics must be lightweight, flexible, and mechanically robust. In wearable applications, it is also preferred to be comfortable and conformal to the body shape; still, it must have resistance to corrosion and have high conversion efficiency. Currently, a few flexible metal rectennas have been produced. A flexible copper-fabric antenna connected to a rigid rectifier has been introduced for wearable applications.[20] In addition, a silver stretchable antenna linked to a rigid rectifier with potential applications in skin-attachable electronics has been reported.[21] An inkjet-printed flexible metal rectenna has also been demonstrated for IoT applications.[22] In flexible rectennas, metal is usually shaped into thin films to pose high electric conductivity and maintain good flexibility. However, they have high specific gravity and are prone to corrode in a harsh chemical environment. Therefore, rectennas must replace the metal with lighter, flexible, and resistant to corrosion materials for flexible applications from a material point of view. Thus, carbon materials are one potential candidate to solve this problem. Graphene is a rising star of carbon materials due to its outstanding conductivity and other unique electrical properties, enabling many applications. However, mono- or few-layer graphene sheets exhibit very high surface resistance and relatively low conductivity at a low microwave frequency band, significantly limiting graphene applications in passive microwave components.[23] With the development of graphene exfoliation techniques in the last few years, more graphene-based materials have been produced on a large scale and at a low cost. Currently, multilayer graphene inks have been reported to provide an option to fabricate rectenna on a flexible substrate via spraying, screen printing, and inkjet-printing

Dr. J. Zhang, Y. Wang, Dr. R. Song, Prof. D. He
Hubei Engineering Research Center of RF-Microwave Technology and Application, School of Science, Wuhan University of Technology, Wuhan 430070, China
E-mail: rongguo_song@whut.edu.cn
E-mail: hedaping@whut.edu.cn
Dr. J. Zhang, Prof. D. He
Sanya Science and Education Innovation Park of Wuhan University of Technology, Sanya 572000, China
Dr. Z. Kou
State Key Laboratory of Advanced Technology for Materials Synthesis and Processing, Wuhan University of Technology, Wuhan 430070, China
The ORCID identification number(s) for the author(s) of this article can be found under https://doi.org/10.1002/eem2.12548.

DOI: 10.1002/eem2.12548

techniques.[24] The graphene flakes in this conductive pattern are compressed to pile sequentially, but gaps are still between the edge of the flakes, which degrade the contact quality. Therefore, the maximum conductivity of the graphene ink is around 7×10^4 S m^{-1}, which severely limits rectenna conversion efficiency. Our group first presented integrated highly flexible graphene macroscopic films (FGMFs) with a stable mechanical ability, high flexibility, and high electrical conductivity (1×10^6 S m^{-1}).[17,18,25] This film is an excellent choice to replace metals in rectenna designs, and some RF devices have been designed and fabricated using integrated multilayer graphene film.

In this work, the design of a laser-fabricated FGMFs-based rectenna is presented to realize omnidirectional wireless energy harvesting from various widely available wireless sources (e.g., LTE, Wi-Fi, microwave oven, and 5G). In addition, we connected the high-efficiency flexible rectenna with a power management unit to continuously supply DC power in various bending conditions to light LEDs. We also present a wearable 2.45 GHz AMC-backed rectenna with potential applications in body-centric wireless sensors. The proposed wearable antenna is demonstrated and successfully harvests wireless energy from a microwave oven to power a sensor. To the best of our knowledge, the graphene-film-based rectennas are first time realized and demonstrated as a power supply for sensors.

2. Characterization of Highly Conductive Graphene Film

The photograph of the prepared FGMFs is shown in **Figure 1**a. It is easy to find that our graphene film has outstanding flexibility. Morphological features of the FGMFs were investigated using a field emission scanning electron microscope (FESEM; JEOL JSM-7610F), and the result is plotted in Figure 1b. The FGMFS is assembled by layers of oriented stacking graphene. X-ray diffraction (XRD) and Raman spectroscopy were used to investigate the quality of FGMFs. As shown in Figure 1c, a sharp and robust diffraction peak of (002) plane located at 26.5° indicates that the interlayer space of stacked multilayer graphene is 0.34 nm. The diffraction peak of (004) plane demonstrates a high graphitization structure of the FGMFS. Raman spectra patterns were recorded and are inserted in Figure 1c, suggesting a sharp diffraction G peak at 1585 cm^{-1} and no obvious D peak at 1335 cm^{-1}. The dropping intensity ratio of the D band and G band (ID/IG) is 0.057, indicating that the proposed FGMFs have high sp^2 hybridized carbon atoms and few lattice defects. The electrochemical behavior (Figure S1, Supporting Information) of the FGMF is also tested using an electrochemical workstation (CH Instruments Ins, CH7601). The tensile strength and resistance to extension of the FGMFs are shown in Figure S2, Supporting Information. In addition, the four-probe method is used to evaluate the electrical conductivity of the FGMFS, which shows outstanding electrical conductivity (1×10^6 S m^{-1}). The electrical resistance of the FGMFS was also tested via a home-built mechanical bending system. As shown in Figure 1d, the resistivity remains constant upon extensive bending cycles with a bending radius of 10 mm at 1 Hz. Results shown in Figure 1d and Figure S2, Supporting Information prove that our prepared FGMFS has excellent flexibility and stability of resistivity.

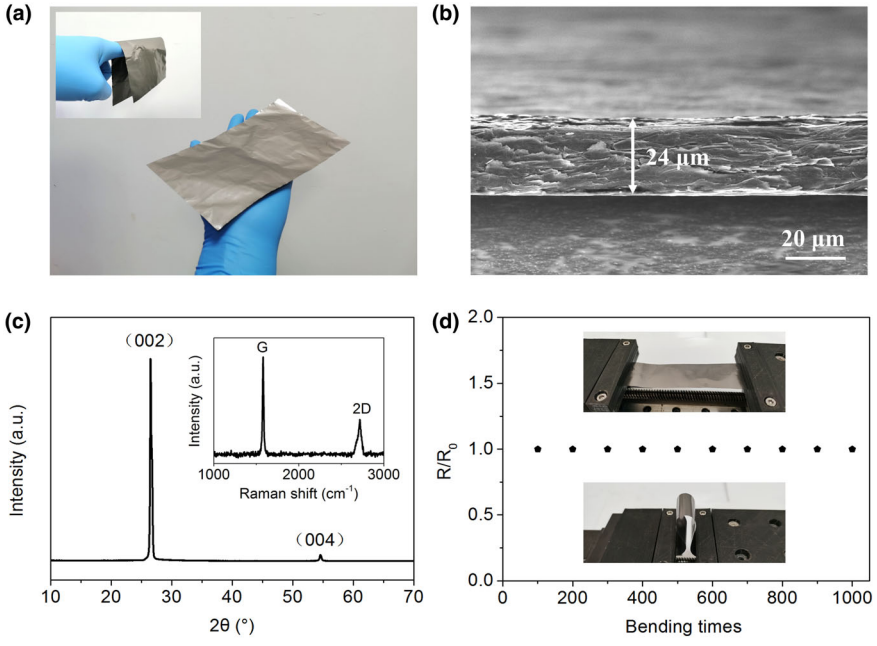

Figure 1. a) Photograph of the fabricated FGMFs. b) SEM image of the fabricated FGMFs. c) Raman spectrum and XRD pattern of the fabricated FGMFs. d) Relative volume resistance of the fabricated FGMFs with a bending test.

3. Rectenna Design

3.1. Flexible Rectifying Circuit

The rectifying circuit is one of the essential parts of a rectenna system, converting the received alternate current (AC) power to DC power. Therefore, the performance of the rectifying circuit can significantly affect the conversion efficiency of the entire system. This work modeled shunt diode rectifiers in some most widely used frequency bands, such as ISM 2.45 GHz, LTE bands, and 5G. The graphene-film-based rectifying circuit (GRC) is placed on a flexible polydimethylsiloxane (PDMS) substrate with a thickness of 0.5 mm. The details of the fabrication process are shown in Figure S3, Supporting Information. To achieve the highest RF-to-DC efficiency at wide bandwidth, the GRC is optimized using the ADS simulation software (Figure S4, Supporting Information). The structural parameters of the fabricated GRC can be found in Table S1, Supporting Information. A Schottky diode (Skyworks SMS7630) is used in the GRC, and an SMA connector is linked to the GRC via conductive adhesives (Double-bond chemical DB2013) to measure the reflection coefficient (S_{11}) with an Agilent E5072A Vector Network Analyzer (VNA).

Figure 2a illustrates the S_{11} of the GRC in free space and mounted on the hand, which proves that the curved condition and human

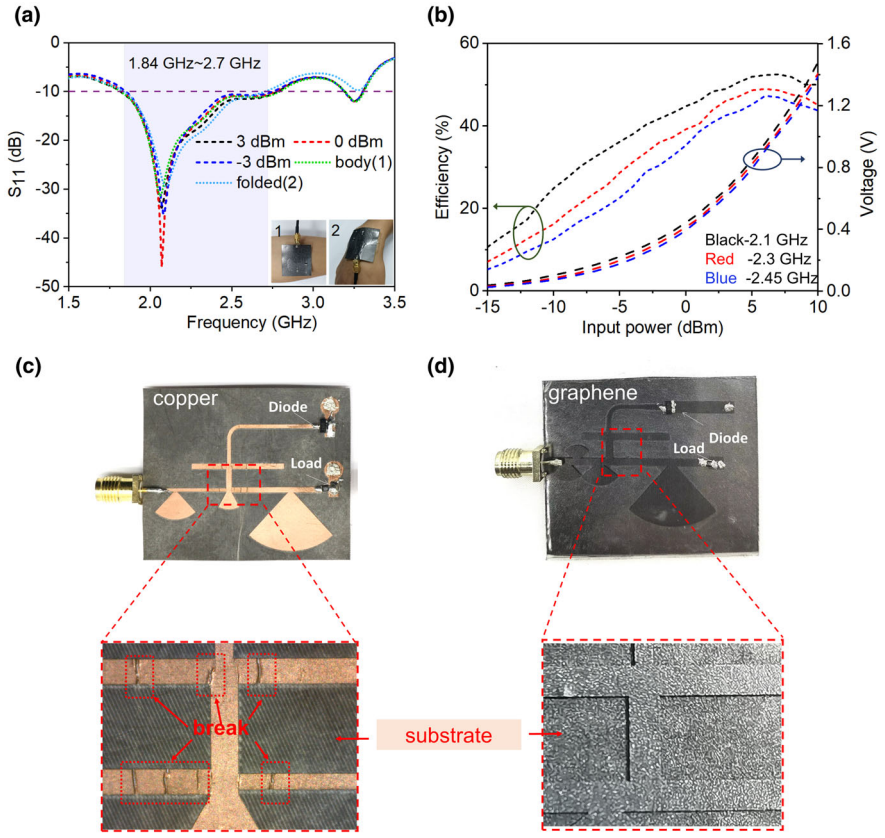

Figure 2. Measurement performance of the GRC. a) Measured reflection coefficient of the GRC in various conditions. b) Measured RF-to-DC efficiency and output voltage of the GRC at 2.1, 2.3, and 2.45 GHz. c) Photographs show a copper-based rectifying circuit after the bending test. d) The GRC after the bending test.

body barely affected the GRC performance. The proposed GRC has a wide impedance bandwidth ($S_{11} < -10$ dB) from 1.84 to 2.7 GHz, which can be very useful for flexible or wearable rectennas at ISM 2.45 GHz (Bluetooth, Microwave oven, Wi-Fi, etc.), LTE, and 5G network. To evaluate the RF-to-DC efficiency of the GRC, we used a signal generator (Agilent N9310A) as a power supplier. We tested the DC output voltage using a multimeter across the load resistor. The RF-to-DC efficiency is obtained by

$$\eta_{\text{rectifier}} = \frac{V^2_{\text{out\_rectifier}}}{R_{\text{load}} P_{\text{in}}} \quad (1)$$

where R_{load} denotes the optimal load resistance (440 Ω) of the GRC and P_{in} is the input power provided by the signal generator. As shown in Figure 2b, at ISM 2.45 GHz, the most common-used free license channel for wireless communications, the peak conversion efficiency is 47% at 8 dBm. The output voltage value is roughly 1.34 V. Furthermore, at LTE communication bandwidth, the peak conversion efficiency is 49% (at 2.3 GHz) and 53% (at 2.1 GHz), respectively. The efficiency decreases after the peak point due to the breakdown effect of the Schottky diode. One of the beauties of using FGMFs to fabricate a rectifying circuit is that the GRC presents more robust flexibility than a traditional metal circuit. Using the same rectifying strategy, we also optimized and fabricated a copper rectifier (with 0.254 mm RT5880 substrate). From the enlarged drawing in Figure 2c, localized fatigue fracture attributed to cyclic stress can be discovered at the transmission line, leading to the failure of the circuit. However, the surface of GRC (Figure 2d) is still smooth and intact even after 200 cycles of repetitive bending. The mechanical stability of the graphene films can significantly increase the service life of the GRC.

3.2. The Flexible Wideband Antenna and the Wearable Antenna

As a core element of a rectenna device, the antenna for wireless energy harvesting typically has unique requirements due to the randomness of the ambient wireless power. A circular monopole antenna is selected due to its wide bandwidth and broad beamwidth, suitable for incoming waves with various frequencies and ambient incident angles, which can harvest more power than a narrowband antenna. As an illustration, we also designed a flexible wideband antenna and a 2.45 GHz wearable antenna for energy harvesting applications. The photograph of these antennas is plotted in **Figure 3**a,b. The structural parameters (as shown in Figures S5a and S6, Supporting Information) of the proposed antenna optimized using CST MWS (Figures S5c,d and S7, Supporting Information) can be found in Tables S3 and S4, Supporting Information.

In flexible devices, the rectenna is expected to be bent or flexed, and we investigate the radiation properties of the antenna, especially the reflection coefficient of the antenna upon bending. To mimic the various bending extends, the proposed antenna is mounted on the surface of cylinders with different radii (Case 1 is r = 28.5 mm; Case 2 is r = 23.5 mm). Figure 3c shows the S_{11} curves of the flexible antenna upon bending deformations. The fraction bandwidth ($S_{11} < -10$ dB) of the flexible wideband antenna is 48.2%, 33.9%, and 25.2% for flat, Case 1, and Case 2, respectively. The dielectric properties of cylinders (Figure S5e, Supporting Information) and the influence of impedance upon bending (Figure S5f, Supporting Information) mainly cause the bandwidth shift in the test. The deformation of the antenna leads to a slight deviation of the resonant frequency and bandwidth. A good agreement in the S_{11} curves (Figure 3c and Figure S5e, Supporting Information) is obtained between simulated and experimental results. In the meantime, radiation patterns (Figure 3e) and gains (Figure S8a, Supporting Information) are measured in the microwave anechoic chamber. Note that the flexible wideband antenna has an omnidirectional radiation pattern and board beamwidth, suitable for ambient wireless energy harvesting.

The antenna needs to operate closely with the human body in wearable devices. The influence of the human body is considered in our investigation. We demonstrate a kind of AMC-backed wearable antenna

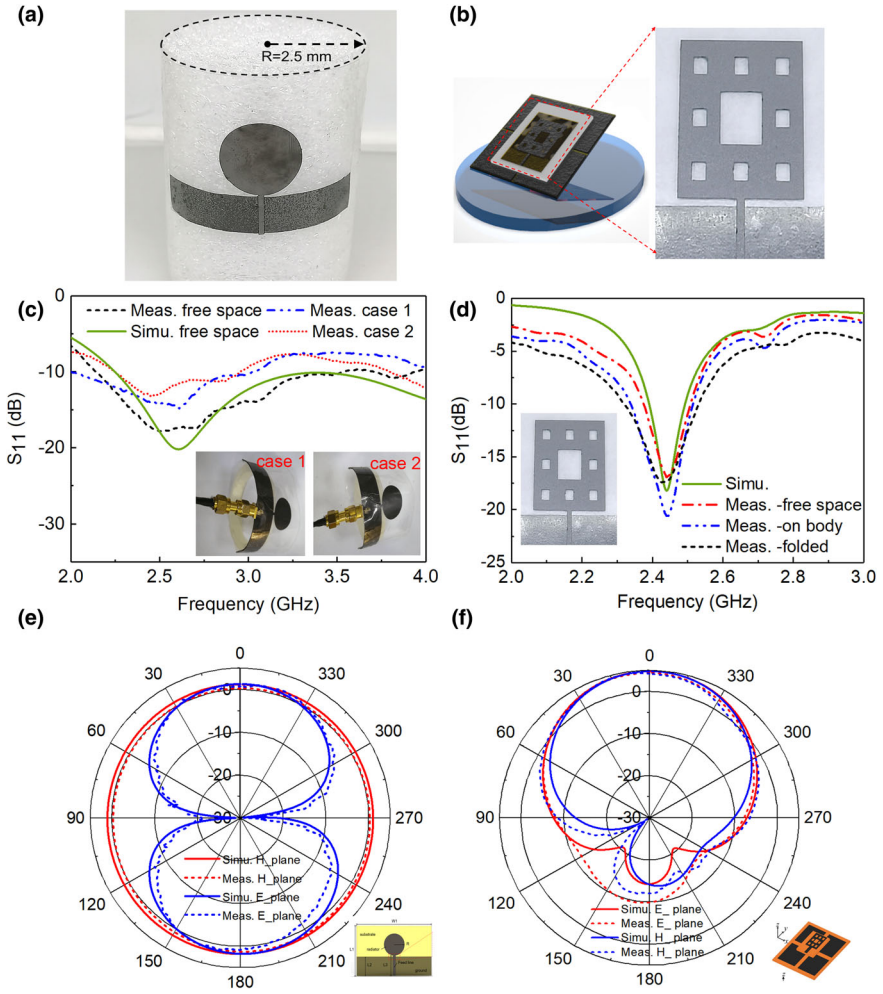

Figure 3. Layout and measurement performance of the wideband flexible antenna and wearable antenna. a) The photograph of the flexible antenna. b) The layout and photograph of the wearable antenna. c) The reflection coefficient of the flexible antenna in various bending conditions. d) The reflection coefficient of the wearable antenna. e) The radiation pattern of the flexible antenna. f) The radiation pattern of the wearable antenna.

(layout see Figure 3b) designed and optimized to harvest wireless power, as shown in Figures S6 and S7, Supporting Information.

An AMC surface (Figure S6, Supporting Information) is realized using a 2 × 2 array of graphene-based AMC unit cells along the lateral *x*- and *y*-axes. Figure 3d shows the influence of on-body and deformation on the radiation properties of the AMC-backed antenna. In addition, the corresponding 2D radiation patterns (Figure 3f) and gains (Figure S8b, Supporting Information) reveal that the highly effective antenna owns unidirectional radiation properties due to the backward waves reflected to the upper half-space by the AMC surface. As shown in Figure 3d, the isolation of the AMC surfaces led to a negligibly small change in the resonant frequency, which supports the durable radiation properties of the antenna in wearable applications.

3.3. Energy Harvesting Rectennas

Connecting the proposed wideband antenna with the GRC yields a wideband rectenna (**Figure 4a**). The proposed rectennas are tested in an anechoic chamber, and the measurement system is shown in Figure S9, Supporting Information. The output DC power in dBm can be calculated by $P_{out} = V_{DC}^2/R_{load}$, where V_{DC} is the measured output voltage of the rectenna and R_{load} is the load resistor. The conversion efficiency of the rectenna equals the output power over the input power by antennas (measured using a spectrum analyzer).

Figure 4b illustrates the measured output voltage and conversion efficiency of the flexible rectenna as a function of the received RF power and frequency. The flexible wideband rectenna shows good performance in wirelessly harvesting the RF power. At 2.1 GHz, the conversion efficiency is about 44.2% at an input power level of 0 dBm. The corresponding output voltage is 0.44 V. Additionally, with the input power level from −10 to 15 dBm, the conversion efficiency of our flexible wideband rectenna still keeps in the range of 24–52% (at 2.1 GHz), 15.7–46% (at 2.3 GHz), and 11–44% (at 2.45 GHz), respectively. Moreover, the rectenna has a wide bandwidth feature (from 2.16 to 2.7 GHz) and works well at the desired input power levels. It is worth noting that the conversion efficiency is high over the wide bandwidth (for Wi-Fi/ISM, LTE, and 5G) of interest. From the view of IoT applications, flexible rectennas can successfully harvest wideband wireless energy and works as a power supply for a low-power device (Figure 4c).

For wearable applications, we integrate the proposed AMC-backed antenna with a 2.45 GHz GRC (Figure S4e,f, Supporting Information) as a demonstration. Figure 4d illustrates the measured output voltage and RF-to-DC conversion efficiency of the wearable rectenna as the received RF power. It can be observed that the wearable rectenna has a maximum conversion efficiency of 55.7%, and the corresponding output voltage can reach 1.56 V for an input power of 8 dBm, which can be further improved by using a low-loss substrate. From the view of wearable applications, the rectified power can be further regulated by a DC–DC boost converter and power management unit for charging supercapacitors or other power storage units. Compared with traditional rectennas, take copper rectennas as an example, the FGMF-based rectenna has some significant advantages on lighter, environmental-friendly, flexible, resistant to corrosion, and good thermal conductivity (Table S5, Supporting Information), which shows great potential for IoT flexible applications. The reported conversion efficiency is also significantly higher than the flexible graphene-based rectenna.[24] The comparison of demonstrated rectennas with previous reports is illustrated in Table S6, Supporting Information. The integrated graphene-film-based rectennas are first time realized and demonstrated with good mechanical stability (Figure S10, Supporting Information) and resistance to corrosion (Figure S11, Supporting Information).

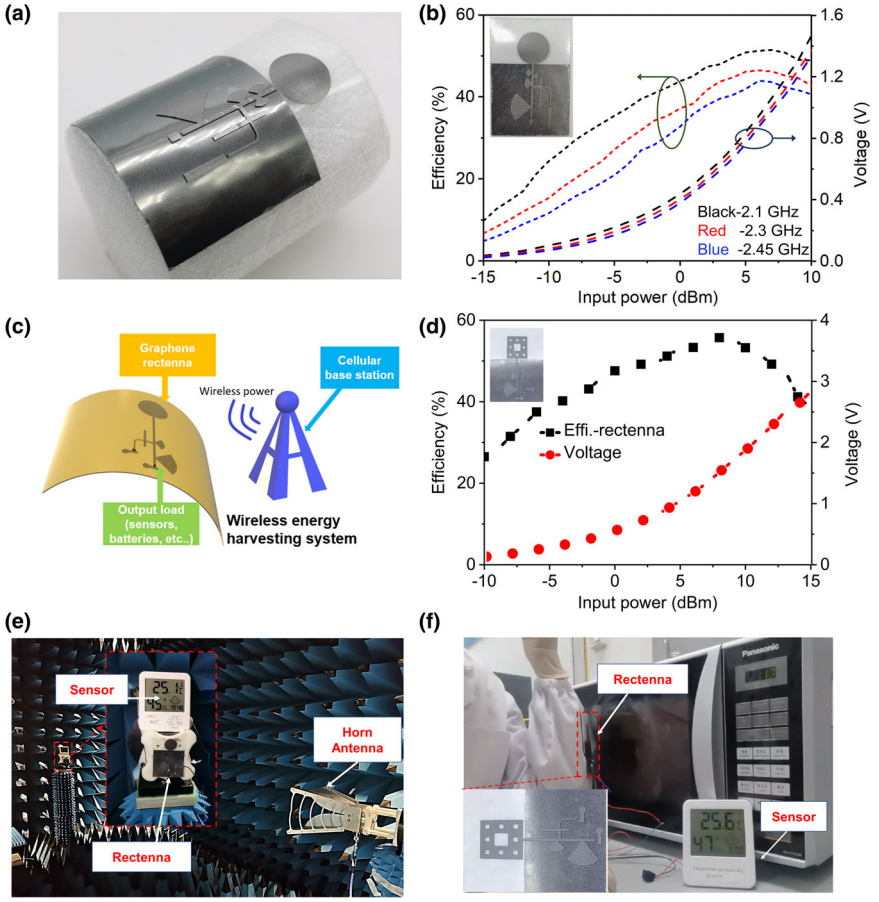

Figure 4. Measurement performance and demonstrations of proposed rectennas. a) Photograph of the flexible rectenna. b) Measured RF-to-DC efficiency and output voltage of the wideband rectenna at 2.1, 2.3, and 2.45 GHz. c) Illustration of wireless energy harvesting system. d) Measured RF-to-DC efficiency and output voltage of the wearable rectenna at 2.45 GHz. e) The demonstration of a flexible wideband rectenna. f) The demonstration of a wearable rectenna system.

We demonstrate a flexible rectenna energy harvesting system (Figure 4e) for a temperature sensor. Due to the excellent stability, the device worked even under wrapped conditions (see Video S1, Supporting Information). In addition, as shown in Figure 4f and Video S2, Supporting Information, we also place a wearable rectenna on our clothes to harvest the ambient wireless energy generated by other devices. The wearable rectenna connects with the power management unit and successfully works as a power supply for sensors.

4. Conclusion

Wireless energy harvesting devices are designed and manufactured using graphene films, which have an outstanding conductivity of 1×10^6 S m^{-1} and good resistive stability. A wideband GRC was optimized using computer modeling to achieve the best conversion efficiency. The results illustrated that the GRC achieves a peak RF-to-DC efficiency of 53%. Also, the GRC was tested to reveal a stable reflection coefficient with body effects. Meanwhile, a flexible wideband monopole antenna is integrated with the GRC to harvest wireless power at ISM 2.45 GHz, LTE, and 5G bands. This wideband rectenna can capture wireless energy from ambient angles and achieve a peak conversion efficiency of 52% at desired frequencies. A 2.45 GHz AMC-backed wearable rectenna is designed, fabricated, and tested to further explore the device in wearable applications, effectively reducing the body effect and showing the maximum conversion efficiency of 55.7% at the ISM band. The results confirm that our design has great potential to perform as a power supplier for flexible and wearable sensors in IoT and other practical applications.

5. Experimental Section

Materials: The homemade FGMFS is processed as follows: Firstly, the graphene oxide (GO) (Wuxi Chengyi Education Technology Co. Ltd) is diluted to 10–20 mg mL^{-1} with ultrapure water to produce a GO suspension. Secondly, GO suspension is stirred and scraped on a PET film. In order to facilitate the removal of the GO film, we coated a layer of silicone oil on the side of the PET substrate. Then, the film is obtained by an evaporative drying process at room temperature for 24 h. Thirdly, the film is annealed at 1300 °C for 2 h and 3000 °C for 1 h, both within an argon atmosphere. Finally, an FGMFS is produced by rolling compression.

Methods: Morphological features of the HCGF were investigated using a field emission scanning electron microscope (FESEM, JEOL JSM-7610F). Raman spectra patterns were recorded by lab PAM HR Evolution Raman Spectrometer, and XRD results were detected on a Rigaku Smartlab SE instrument using Ni-filtered Cu Ka radiation.

For reflection coefficient measurement, the device under test (antenna or rectifying circuit) was directly connected to a calibrated VNA (Agilent E5072A).

The gain-transfer method is used to measure antenna gain in the microwave anechoic chamber. A reference antenna (A-INFO LB-10180), an antenna under test (AUT), and a horn antenna (Hengda Microwave HD-10200DRHA10S) are used. To satisfy the far-field requirement, the measurement distance between any two tested antennas is 2 m. The following equations can obtain the gain of the AUT at every frequency point:

$$G_{AUT} = G_{ref} + G_{relative} \quad (2)$$

$$G_{relative} = S_{21}^{HR} - S_{21}^{AR} \quad (3)$$

where G_{ref} is the gain of the reference antenna. $G_{relative}$ is denoted by the loss of the AUT relative to the reference. S_{21}^{HR} is measured S_{21} (in dB) between horn antenna and reference antenna. S_{21}^{AR} is measured S_{21} (in dB) between the horn antenna and the AUT.

Radiation patterns of the antenna were measured using Diamond Engineering Automated Measurement Systems and VNA (Agilent E5072A). The data were recorded every 3° rotation, and the measurements were made in the microwave anechoic chamber.

Direct current output voltage of the rectenna was measured by using a commercial horn antenna (A-INFO LB-10180) as a transmitter, a signal generator (Agilent N9310A) as a signal source, a 40 dB power amplifier to amplify transmitted power, a spectrum analyzer (Agilent N9320B) to measure the input power and a voltage meter to measure the DC output. The distance between the rectenna under the test to the transmitter is 1 m.

Acknowledgements

This work is supported by the National Natural Science Foundation of China (Grant No. 62001338), the Open Funds for Sanya Science and Education Park (Grant No. 2021KF0018), and the Fundamental Research Funds for the Central Universities (Grant No. WUT:2021IVB029).

Conflict of Interest

The authors declare no conflict of interest.

Supporting Information

Supporting Information is available from the Wiley Online Library or from the author.

Keywords

flexible rectennas, highly flexible graphene-based films, wireless energy harvesting

Received: May 20, 2022
Revised: October 7, 2022
Published online: October 8, 2022

[1] L. Catarinucci, D. D. Donno, L. Mainetti, L. Palano, L. Patrono, M. L. Stefanizzi, L. Tarricone, *IEEE Internet Things J.* **2015**, *2*, 515.
[2] A. Zanella, N. Bui, A. Castellani, L. Vangelista, M. Zorzi, *IEEE Internet Things J.* **2014**, *1*, 22.
[3] X. Zhang, J. Grajal, J. L. Vazquezroy, U. Radhakrishna, X. Wang, W. Chern, L. Zhou, Y. Lin, P. Shen, X. Ji, *Nature* **2019**, *566*, 368.
[4] S. P. Shen, C. Y. Chiu, R. D. Murch, *IEEE Trans. Antennas Propag.* **2018**, *66*, 644.
[5] Y. L. Liu, K. M. Huang, Y. Yang, B. Zhang, *IEEE Antennas Wirel. Propag. Lett.* **2018**, *17*, 1659.
[6] C. Song, Y. Huang, J. Zhou, P. Carter, S. Yuan, Q. Xu, Z. Fei, *IEEE Trans. Ind. Electron.* **2017**, *64*, 3950.
[7] V. Kuhn, C. Lahuec, F. Seguin, C. Person, *IEEE Trans. Microw. Theory Tech.* **2015**, *63*, 1768.
[8] G. Monti, L. Corchia, L. Tarricone, *IEEE Trans. Antennas Propag.* **2013**, *61*, 3869.
[9] C. Song, Y. Huang, P. Carter, J. Zhou, S. Joseph, G. Li, *IEEE Trans. Antennas Propag.* **2018**, *66*, 3306.
[10] J. Zhang, Y. Huang, P. Cao, *Trans. Inst. Meas. Control.* **2015**, *37*, 961.
[11] S. Hemour, Y. Zhao, C. H. P. Lorenz, D. Houssameddine, Y. Gui, C. Hu, K. Wu, *IEEE Trans. Microw. Theory Tech.* **2014**, *62*, 965.
[12] C. Song, P. Lu, S. Shen, *IEEE Trans. Ind. Electron.* **2020**, *68*, 8128.
[13] P. Wu, S. Y. Huang, W. Zhou, Z. H. Ren, Z. Liu, K. Huang, C. Liu, *IEEE Microw. Wirel. Compon. Lett.* **2018**, *28*, 1116.
[14] Y. Y. Shi, J. W. Jing, Y. Fan, L. Yang, J. F. Pang, M. Wang, *Microw. Opt. Technol. Lett.* **2018**, *60*, 2420.
[15] A. Saffari, M. Hessar, S. Naderiparizi, J. R. Smith, Presented at *2019 IEEE Int. Conf. RFID (RFID)*, USA **2019**, 4.
[16] V. Talla, B. Kellogg, S. Gollakota, J. R. Smith, Presented at *Proc. ACM Int. Joint Conf. Pervasive Ubiquitous Comput. (UBICOMP)*, Hawaii **2017**, 9.
[17] W. Zhou, C. Liu, R. Song, X. Zeng, B.-W. Li, W. Xia, J. Zhang, G.-L. Huang, Z. P. Wu, D. He, *Appl. Phys. Lett.* **2019**, *114*, 113503.
[18] D. Tang, Q. Wang, Z. Wang, Q. Liu, B. Zhang, D. He, Z. Wu, S. Mu, *Sci. Bull.* **2018**, *63*, 574.
[19] X. Huang, T. Leng, X. Zhang, J. C. Chen, K. H. Chang, A. K. Geim, K. S. Novoselov, Z. Hu, *Appl. Phys. Lett.* **2015**, *106*, 203105.
[20] S. Adami, P. Proynov, G. S. Hilton, G. Yang, C. Zhang, D. Zhu, Y. Li, S. P. Beeby, I. J. Craddock, B. H. Stark, *IEEE Trans. Microw. Theory Tech.* **2018**, *66*, 380.
[21] J. Zhu, Z. Hu, C. Song, N. Yi, Z. Yu, Z. Liu, S. Liu, M. Wang, M. G. Dexheimer, J. Yang, H. Cheng, *Mater. Today Phys.* **2021**, *18*, 100377.
[22] A. Eid, J. G. D. Hester, J. Costantine, Y. Tawk, A. H. Ramadan, M. M. Tentzeris, *IEEE Trans. Antennas Propag.* **2020**, *68*, 2621.
[23] A. Scidà, S. Haque, E. Treossi, A. Robinson, S. Smerzi, S. Ravesi, S. Borini, V. Palermo, *Mater. Today* **2018**, *21*, 223.
[24] K. Pan, Y. Fan, T. Leng, J. S. Li, Z. Xin, J. Zhang, L. Hao, J. C. Gallop, K. S. Novoselov, Z. Hu, *Nat. Commun.* **2018**, *9*, 1.
[25] R. Song, G.-L. Huang, C. Liu, N. Zhang, J. Zhang, C. Liu, Z. P. Wu, D. He, *Int. J. RF Microw. Comput.-Aided Eng.* **2019**, *29*, e21692.